Nanoparticle Hybrids

DOI: 10.1002/anie.201101833

Platinum Nanoparticles Encapsulated by Aminopeptidase: A Multifunctional Bioinorganic Nanohybrid Catalyst**

*Boi Hoa San, Sungsu Kim, Sang Hyun Moh, Hyunjoo Lee, Duk-Young Jung, and Kyeong Kyu Kim**

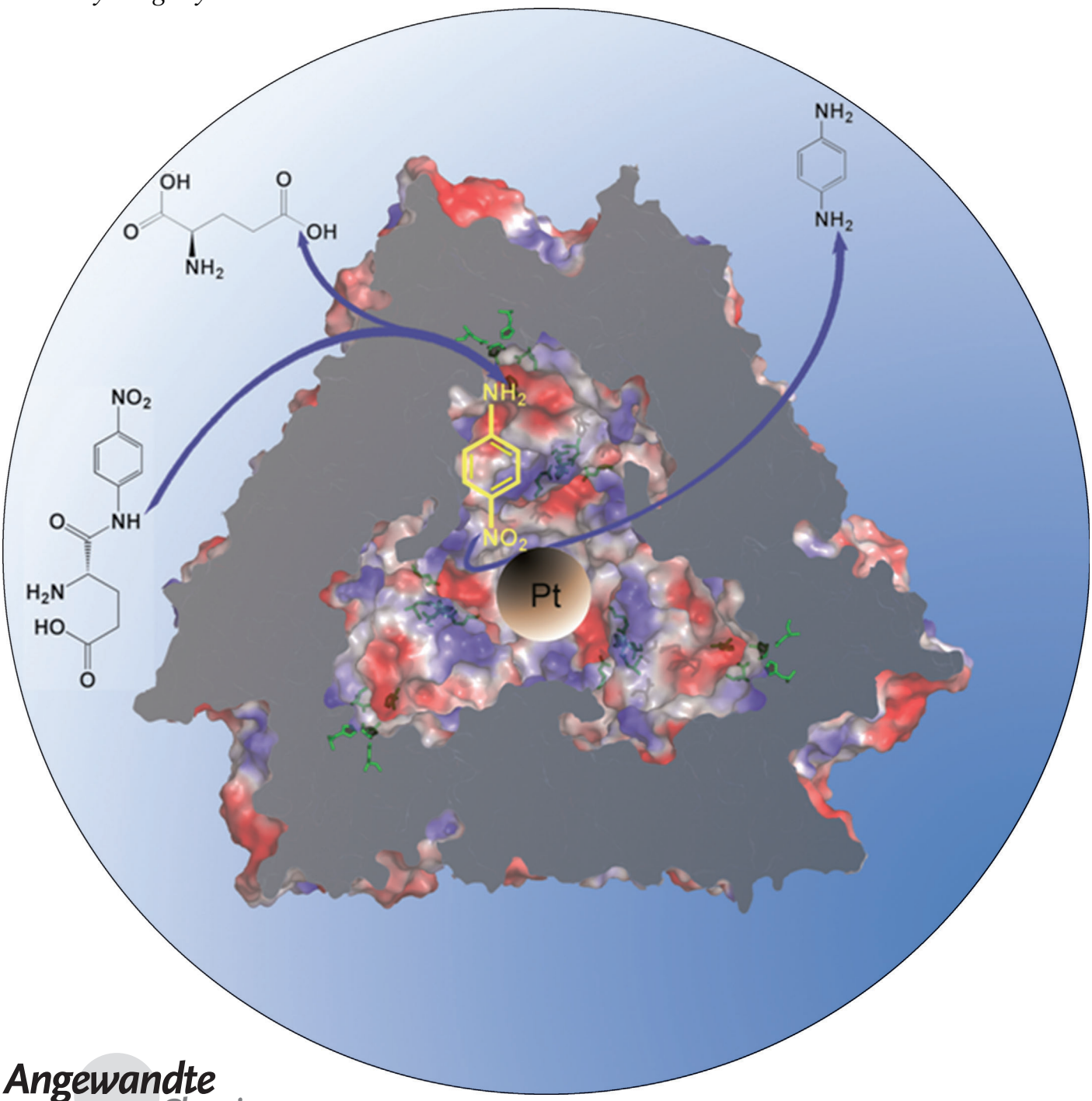

Biomineralization synthesis of metallic nanoparticles using biotemplates has been the theme of numerous investigations,[1] since it allows for the production of high-quality nanoparticles by altering the physical properties of the prepared inorganic materials at the ambient temperature. Most notably, biomineralization using protein shells (PSs) or cages is being intensely studied for the synthesis of inorganic nanomaterials that can be applied to electromagnetic devices, photonics, catalysts, and a variety of other fields.[2] Furthermore, the functional modification of protein surfaces by genetic or chemical means[3] expands the repertoire of applying inorganic nanomaterials to medical imaging and therapy.[3b,4] However, most applications of protein-shelled nanoparticles (PSNPs) are still limited to their inorganic properties, and the role of PSs is restricted to that of a reservoir or, at most, a targeting entity for a specific location, such as the cell surface.[3b,5] Herein, by employing peptidases as PSs, we demonstrate that the catalytic activities of both the proteins and NPs can be combined for multistep synthesis of the desired compounds. Furthermore, we show that our PSs are ideal templates for the size-controlled synthesis of ultrasmall platinum nanoparticles (PtNPs) within the size range of 0.9–3.2 nm, and that they have higher catalytic capacities with biocompatibility.

The bacterial aminopeptidase from *Streptococcus pneumonia* (PepA) self-assembles into a well-defined tetrahedral dodecameric complex with a diameter of about 12 nm at the exterior and 6 nm at the interior (Figure 1 a, b). PepA is a zinc-dependent metallopeptidase with a substrate preference for acidic amino acids,[6] and it plays an important role in catabolizing oligopeptides in bacteria. The active sites located inside the cavity hydrolyze oligopeptides into free amino acids. The tetrahedral architecture of PepA reveals a cavity in the center with four wide channels on the faces of the tetrahedron and four narrow ones on the edges (Figure 1 a). The wide and narrow channels have diameters of 3 and 1 nm, respectively, and they are used for substrate entry and product exit, respectively. Accordingly, these channels are considered the gates for accepting inorganic molecules during the PtNP synthesis. The negatively charged interior surface seems to be crucial for metal deposition in the initial stage of the reaction (Figure 1 b). The geometric and electrostatic complementarity among each subunit results in very tight subunit interaction. Owing to these features, PepA is considered an ideal biotemplate for the synthesis of inorganic nanoparticles (Figure 1 b).

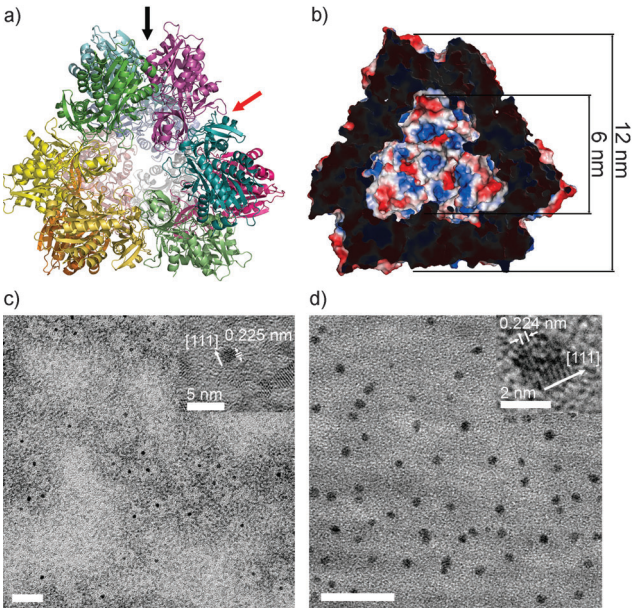

Figure 1. Crystal structure (PDB ID: 3KL9) and TEM images of PepA. a) The ribbon diagram of a PepA dodecamer. The PepA subunits are shown in different colors, and the channels with diameters of 1 and 3 nm are indicated by black and red arrows, respectively. b) The charge distribution on the internal surface of PepA: negative charges are red and positive charges are blue, and the inside and outside dimensions are indicated. c,d) PepA–PtNP complexes were analyzed using electron microscopy with 2% uranyl acetate staining (c) and without staining (d). The insets are magnified images of the uranyl acetate-stained PepA–PtNP complexes (c) and PtNPs (d). The lattice fringes show periodicities of 0.224 (c) and 0.225 nm (d) in the [111] direction (white arrows). Scale bars are 20 nm unless otherwise noted.

PtNPs were synthesized within PepA by slowly reducing K_2PtCl_4 using $NaBH_4$ as a reducing agent in an aqueous solution at room temperature. The synthesis was monitored using transmission electron microscopy (TEM) (Figure 1 c, d) and UV/Vis spectroscopy (Figure 2). The formation of PtNPs was also visibly monitored by color change from light yellow to dark brown (Figure S1, Supporting Information). Consistent with other studies,[7] PepA–PtNPs showed broad UV/Vis absorption spectra in a wide range of wavelengths, but there were no peaks corresponding to the absorption of $PtCl_4^{2-}$ or the plasmon absorption. UV absorption at 280 nm, which is a representative fingerprint of proteins, did not shift, but rather, it gradually increased in intensity and was finally saturated, implying that the formation of PepA–PtNPs was kinetically controlled (Figure 2). PepA–PtNPs were purified using high-speed centrifugation and size-exclusion chromatography (SEC). The TEM images of PepA–PtNPs stained with 2% uranyl acetate revealed uniform round PtNPs encapsulated in

[*] B. H. San, S. H. Moh, Prof. Dr. K. K. Kim
Department of Molecular Cell Biology
Samsung Biomedical Research Institute
Sungkyunkwan University School of Medicine
Suwon 440-746 (South Korea)
E-mail: kkim@med.skku.ac.kr
Homepage: http://smsb1.skku.ac.kr/index.html
B. H. San, S. H. Moh, Prof. Dr. D.-Y. Jung, Prof. Dr. K. K. Kim
Sungkyunkwan Advanced Institute of Nanotechnology
Sungkyunkwan University, Suwon 440-746 (South Korea)
Prof. Dr. D.-Y. Jung
Department of Chemistry-BK21-SAINT, Institute of Basic Sciences
Sungkyunkwan University, Suwon 440-746 (South Korea)
S. Kim, Prof. Dr. H. Lee
Department of Chemical and Biomolecular Engineering
Yonsei University, Seoul 120-749 (South Korea)

[**] This work was supported by the Next-Generation BioGreen 21 Program (SSAC PJ008107).
Supporting information for this article is available on the WWW under http://dx.doi.org/10.1002/anie.201101833.

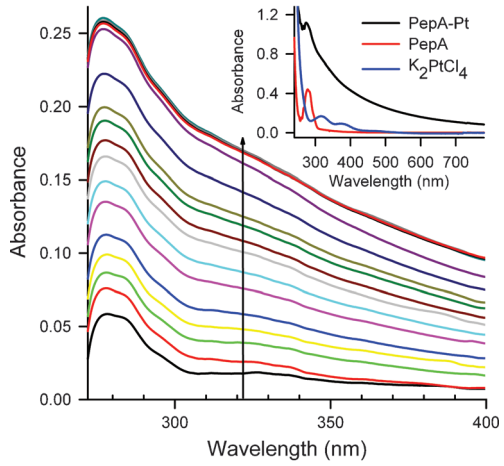

Figure 2. UV/Vis spectra of PepA–PtNPs in the 250–400 nm range. PepA and Pt precursors were incubated at a 1:1000 molar ratio. The spectra obtained from the incubation of 0, 1, 2, 3, 5, 10, 15, 20, 25, 30, 35, 40, 45, 50, 55, 60, and 120 min are differently colored. The absorption spectra appeared saturated after about 50 min, indicating the termination of the reaction. The inset panel shows the UV/Vis spectra of PepA, the Pt precursors, and PepA–PtNP complexes over the spectral range of 250–800 nm.

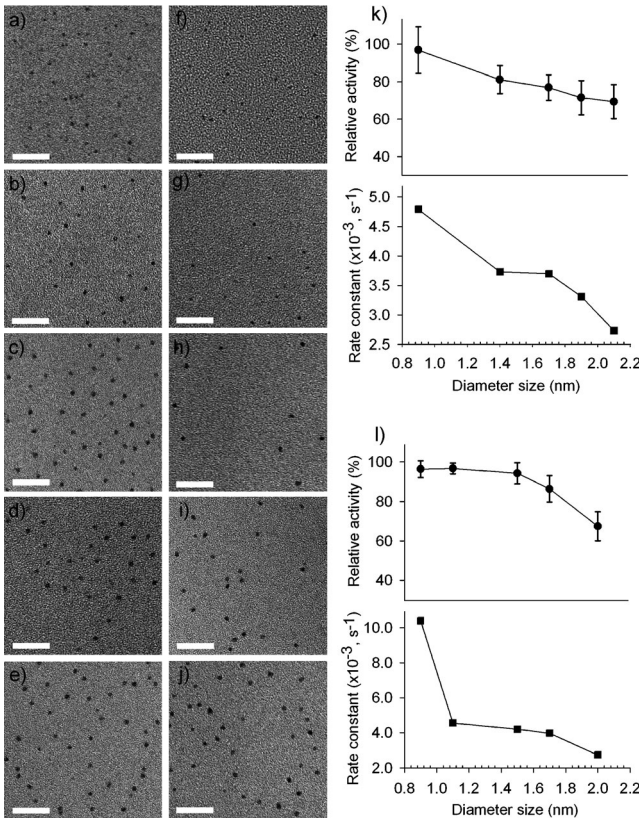

Figure 3. The size-controlled evolution of the PepA-encapsulated PtNPs and their catalytic activities. a–e) Kinetically controlled synthesis of PepA–PtNPs. Pt precursors were incubated with PepA at a 1000:1 molar ratio. Varying incubation times of 1 (a), 5 (b), 15 (c), 30 (d), and 5 h (e) yielded average complex sizes of 0.9, 1.4, 1.7, 1.9, and 2.1 nm, respectively (size distribution histogram, Figure S8, Supporting Information). f–j) Ratio-controlled synthesis of PepA–PtNPs. Pt precursors were incubated with PepA at varying molar ratios of 50:1 (f), 100:1 (g), 250:1 (h), 500:1 (i), and 1000:1 (j) for 60 min, yielding average complex sizes of 0.9, 1.1, 1.5, 1.7, and 2.0 nm, respectively (size distribution histogram, Figure S9, Supporting Information). Each scale bar represents 20 nm. The proteolysis and hydrogenation activities of the PepA–PtNP complexes synthesized in a–e and f–j are plotted versus the size of PtNPs ((k) and (l), respectively; Figure S10 and Figure S11, Supporting information). The proteolytic activity of PepA–PtNPs was monitored by the hydrolysis of substrates over 15 min at 37 °C, expressed as the relative activity to free PepA. The hydrogenation activity is denoted by the rate constant.

tetrahedral PepA shells (Figure 1 c). The molar ratio between the Pt precursors and PepA and the incubation time determined the size of PtNPs encapsulated by PepA. When a reaction mixture with a molar ratio of 1000:1 was incubated until the Pt precursors were completely reduced, PtNPs with diameters of (2.1 ± 0.3) nm were synthesized inside of PepA, and these were used for the physicochemical characterization. The lattice spacing of the crystalline PtNPs was 0.224 nm, which can be assigned to the (111) plane of fcc platinum (Figure 1 d). Therefore, the crystalline property of PtNPs synthesized by PepA is same as that of PtNPs encapsulated by other protein shells such as ferritin,[7b] DNA-binding protein of starved cells (Dps),[8] and small heat-shock protein (sHSP).[2b] The inductively coupled plasma mass spectrometry (ICP-MS) analysis confirmed that PepA possess smaller amounts of zinc ions after harboring PtNPs, suggesting that the zinc ions bound to the active site of PepA were released or replaced by platinum ions (Table S1, Supporting Information). The SEC profiles of the apo-PepA and PepA–PtNP complexes monitored at 280 and 350 nm revealed that the major peaks were eluted at the same volume, thus confirming that Pt was deposited within the PepA dodecamers and not on their surfaces (Figure S2, Supporting Information). Fourier-transform infrared (FTIR) spectroscopy and X-ray photoelectron spectroscopy (XPS) revealed the binding sites of PtNPs in PepA and the metallic state of the deposited Pt (Figures S3 and S4; Table S2, Supporting Information).

The size of PtNPs was precisely controlled in the range of 0.9 to 2.1 nm by changing either the reaction time (kinetically controlled synthesis; Figure 3 a–e) or the concentration ratio between Pt precursors and proteins (ratio-controlled synthesis; Figure 3 f–j). The size of PtNPs increased up to 3.2 nm when PepA was saturated with excess Pt precursor (Figure S5, Supporting Information). Smaller nanoparticles are known to possess higher catalytic activity,[9] but the synthesis of ultrasmall PtNPs at a subnanometer scale is a challenging issue. To date, only a few investigations have addressed the kinetic effects in the size control of PtNPs[10] or the synthesis of ultrasmall PtNPs,[11] but those efforts were rather limited and impractical. In this regard, the current study provides a simple and reliable technique for the synthesis of ultrasmall PtNPs that are smaller than any other known PtNPs produced in ambient conditions.[10] Collectively, it is believed that the tetrahedral protein shell of PepA is an attractive biotemplate for the syntheses of ultrasmall inorganic nanoparticles.

The peptidase activity of the PepA–PtNPs was monitored in two ways: the amount of released of *p*-nitroanilide from glutamic acid-*p*-nitroanilide for 15 min was measured (Fig-

ure 3k,l), and the ration of the catalysis rate constant to the Michaelis constant (k_{cat}/K_m) of PepA was calculated (Table 1). As confirmed in the ICP-MS experiments, PepA–PtNPs

Table 1: Peptidase and hydrogenation activities of PepA–PtNPs.

	Peptidase activity k_{cat}/K_m [$mM^{-1}s^{-1}$]	Hydrogenation activity rate constant [$10^{-3}s^{-1}$]
PepA	14.88 ± 0.45	–
PepA–PtNP ca. 0.9 nm	6.29 ± 0.49	10.400
PepA–PtNP ca. 1.0 nm	4.30 ± 0.02	4.552
PepA–PtNP ca. 1.5 nm	3.50 ± 0.06	4.200
PepA–PtNP ca. 2.0 nm	1.66 ± 0.01	2.730

contained a smaller amount of zinc ions than the Pt-free PepA, but they still have the high peptidase activity of PepA–PtNPs, possibly owing to the bound zinc and platinum ions. The reaction rate constant of PepA–PtNPs-catalyzed hydrogenation was also estimated using *p*-nitrophenol as a substrate. Since PepA–PtNPs produced from the Pt/protein ratio-controlled synthesis were catalytically more active (Figure 3l) than those from the kinetic controlled synthesis (Figure 3k), their activity is referred to in the discussion, unless otherwise specified. PepA–PtNPs showed higher catalytic activity than the citrate-reduced PtNPs[12] or the Tween80-capped PtNPs[13] of equivalent sizes (Figure S6 and Figure S7, Supporting Information). The peptidase and hydrogenation activities were both inversely proportional to the particle size (Figure 3 and Table 1), and the sub-nanometer-sized PepA–PtNPs were the most efficient catalysts: the proteolytic activity of PepA–PtNPs was comparable to that of the free PepA in terms of the amount of released product during a assigned time, and the hydrogenation activity was fourfold higher than that of the 2 nm PtNPs (Figure 3l). Because they function as an enzyme and a chemical catalyst, PepA–PtNPs can be denoted as a bioinorganic nanohybrid catalyst. At the same time, PepA exerted strong stabilizing effects on PtNPs, since PepA extended the lifespan of PtNPs more effectively than two other representative molecular capping agents (citrate and Tween80, Figure 4a). Furthermore, PepA–PtNPs also exhibited both sorts of activity in organic solvents (Figure 4b), implying that the diversity of the catalytic conditions may contribute to expanding the repertoire of applications for this multifunctional nanocatalyst.

The PepA complexes harboring the 0.9 nm PtNPs, which possessed the highest catalytic activity, appear to be suitable for various application purposes. In similar ways, PepA can possibly be applied to synthesize various inorganic catalytic materials that have high catalytic activity, as PSs have been successfully used for the synthesis of a wide range of inorganic nanoparticles.[1a,c,d,2b,3c,4,14] Moreover, PepA–PtNPs showed no detectable toxicity on cultured cells in the MTT assay, which is unlike PtNPs stabilized by Tween80, suggesting that PepA can reduce the cytoxicity of PtNPs (Figure 4c). Inorganic materials may acquire biocompatibility through PepA encapsulation, which is essential for the biomedical application of nanomaterials. Consistently, it was also confirmed that the catalytic reactions do not affect the conformational integrity of PepA–PtNPs, since the SEC profile of PepA–PtNPs was not changed after multiple reactions either in water (Figure S2, Supporting Information) or in organic solvents (data not shown).

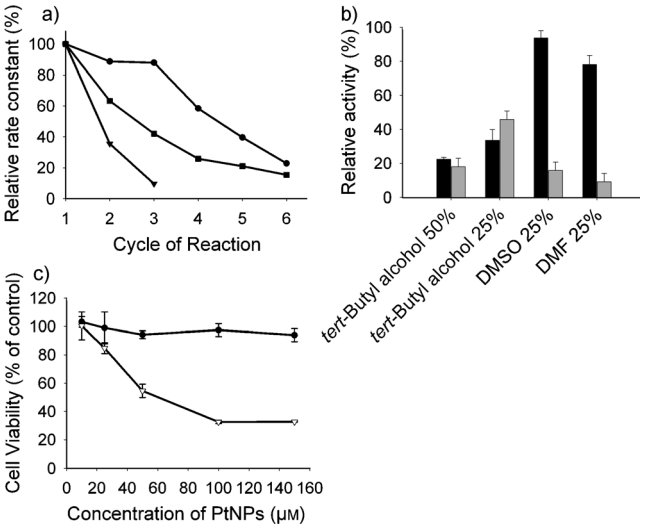

Figure 4. The lifespan catalytic activity of PepA–PtNPs, their activity in organic solvents, and their biocompatibility. a) Catalytic activities of PepA–PtNPs (●), citrate–PtNPs (▼) and Tween80–PtNPs (■) with equivalent diameters (2 nm) in a multiple-cycle reaction. The catalytic activity of each of the PtNPs, as expressed by the rate constant of the first reaction, was set to 100%, and the relative activities of the next reactions were plotted. b) The hydrolysis (black) and hydrogenation (gray) activities of PepA–PtNPs in 50% and 25% *tert*-butyl alcohol, 25% DMSO (dimethyl sulfoxide), and 25% DMF (dimethyl formamide) are shown relative to the activity in an aqueous solution. c) Cell viabilities in the presence of PepA–PtNPs (●) or Tween80–PtNPs (▽). (3-(4,5-Dimethylthiazol-2-yl)-2,5-diphenyltetrazolium bromide (MTT) assays were performed using Chinese hamster ovary (CHO) cells grown with varying concentrations (10, 25, 50, 100, and 150 μM) of PepA–PtNPs or Tween80–PtNPs. Values represent the means ± standard deviation from six experiments.

The catalytic activities of PepA and PtNPs were tested simultaneously using Glu-*p*-nitroanilide as a substrate. PepA-mediated hydrolysis yielded *p*-nitroanilide, with the development of yellow color (Figure 5). Subsequent hydrogenation of *p*-nitroanilide was monitored by the disappearance of visible color under reduction conditions. When incubated with the PepA–PtNP complex and $NaBH_4$, Glu-*p*-nitroanilide instantly formed the final product *p*-phenylenediamine, thus demonstrating that this two-step reaction was completed by the bioinorganic nanohybrid catalyst.

Although PSs have previously served as templates and carriers in the synthesis and transfer of inorganic nanoparticles,[1a,e,3a,15] they have not been considered as active components. Herein, PepA was catalytically active and functional even with PtNPs deposited inside. PepA could be an excellent component of robust biomaterial, as it not only performs the enzymatic function but also stabilizes the performance of inorganic catalysts and substantially reduces the cytoxicity of PtNPs. In these regards, PepA–PtNPs are differentiated from the other known bioinorganic hybrids, which are mostly simple conjugates of biomolecules and

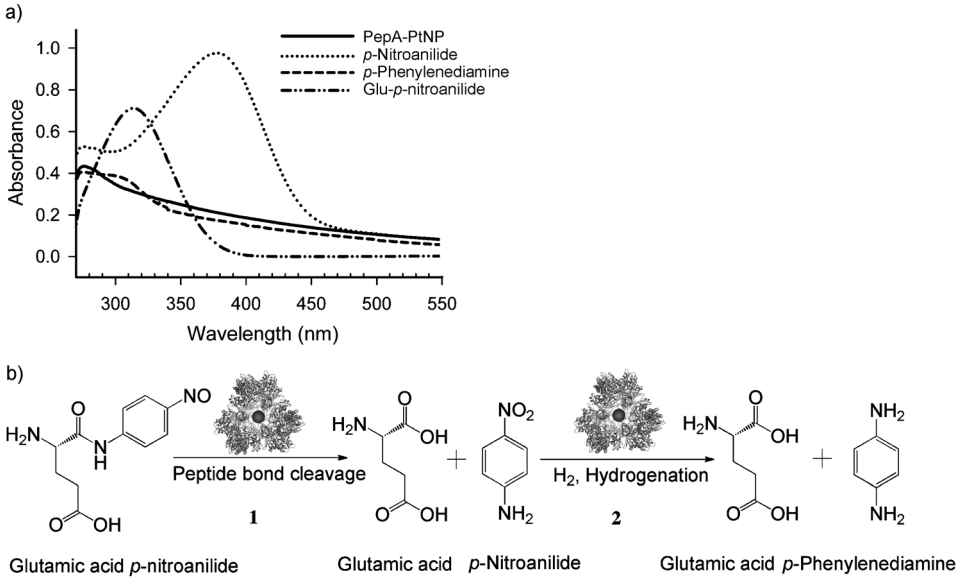

Figure 5. The multistep reaction catalyzed by the PepA–PtNP complexes. a) Hydrolysis of Glu-*p*-nitroanilide (dash dotted line) to *p*-nitroanilide (dotted line) was monitored by the change in the absorption peak from 310 to 380 nm. Subsequent hydrogenation of *p*-nitroanilide to *p*-phenylenediamine resulted in the disappearance of the absorption peak at 380 nm and the emergence of a new peak at 305 nm (dashed line). A solid line indicates the absorption spectrum of the PepA–PtNP complexes. b) Reaction schemes for the PepA–PtNP-catalyzed productions of *p*-phenylenediamine from Glu-*p*-nitroanilide by proteolysis (1) and hydrogenation (2). Glutamic acids were not hydrogenated under the experimental conditions.

inorganic nanomaterials. Moreover, the use of PepA facilitated stringent control over the size of nanoparticles, which enabled us to reproducibly synthesize PtNPs with diameters ranging from 0.9 to 3.2 nm. Therefore, with these advantages, PepA surpasses the other known PSs for designing new functional materials.[1a,e,3a,16] Considering the higher biocompatibility of PepA–PtNPs and the functionality of PSs acquired by genetic or chemical modification of proteins, it is expected that the current study can be extended to the construction of nanobiofactories to produce complex molecules for the purpose of biomedical application. In a similar approach, various inorganic catalysts could be combined with enzymes with PS-like architectures, such as oligomeric acyltransferases,[17] aldolases,[18] decarboxylases,[19] and pyrophosphatases,[20] to diversify the repertoires of bioinorganic nanohybrids for the synthesis of chemical compounds. Considering the increasing demand for enzymes to perform in organic synthesis,[21] this study could expand the scope of synthetic organic chemistry in either aqueous or organic solvents.

Received: March 15, 2011
Revised: June 16, 2011
Published online: September 1, 2011

Keywords: aminopeptidase · bioinorganic catalysts · nanoparticles · platinum · protein shells

[1] a) F. C. Meldrum, V. J. Wade, D. L. Nimmo, B. R. Heywood, S. Mann, *Nature* **1991**, *349*, 684; b) F. C. Meldrum, B. R. Heywood, S. Mann, *Science* **1992**, *257*, 522; c) S. Mann, D. D. Archibald, J. M. Didymus, T. Douglas, B. R. Heywood, F. C. Meldrum, N. J. Reeves, *Science* **1993**, *261*, 1286; d) T. Douglas, D. P. Dickson, S. Betteridge, J. Charnock, C. D. Garner, S. Mann, *Science* **1995**, *269*, 54; e) T. Douglas, M. Young, *Nature* **1998**, *393*, 152.

[2] a) B. Dragnea, C. Chen, E. S. Kwak, B. Stein, C. C. Kao, *J. Am. Chem. Soc.* **2003**, *125*, 6374; b) Z. Varpness, J. W. Peters, M. Young, T. Douglas, *Nano Lett.* **2005**, *5*, 2306; c) R. J. Tseng, C. Tsai, L. Ma, J. Ouyang, C. S. Ozkan, Y. Yang, *Nat. Nanotechnol.* **2006**, *1*, 72.

[3] a) M. L. Flenniken, D. A. Willits, S. Brumfield, M. J. Young, T. Douglas, *Nano Lett.* **2003**, *3*, 1573; b) M. Uchida, M. L. Flenniken, M. Allen, D. A. Willits, B. E. Crowley, S. Brumfield, A. F. Willis, L. Jackiw, M. Jutila, M. J. Young, T. Douglas, *J. Am. Chem. Soc.* **2006**, *128*, 16626; c) H. Wu, J. Wang, Z. Wang, D. R. Fisher, Y. Lin, *J. Nanosci. Nanotechnol.* **2008**, *8*, 2316.

[4] J. F. Hainfeld, *Proc. Natl. Acad. Sci. USA* **1992**, *89*, 11064.

[5] M. L. Flenniken, D. A. Willits, A. L. Harmsen, L. O. Liepold, A. G. Harmsen, M. J. Young, T. Douglas, *Chem. Biol.* **2006**, *13*, 161.

[6] D. Kim, B. H. San, S. H. Moh, H. Park, D. Y. Kim, S. Lee, K. K. Kim, *Biochem. Biophys. Res. Commun.* **2010**, *391*, 431.

[7] a) J. A. Creighton, D. G. Eadon, *J. Chem. Soc. Faraday Trans.* **1991**, *87*, 3881; b) J. Fan, J. J. Yin, B. Ning, X. Wu, Y. Hu, M. Ferrari, G. J. Anderson, J. Wei, Y. Zhao, G. Nie, *Biomaterials* **2011**, *32*, 1611.

[8] S. Kang, J. Lucon, Z. B. Varpness, L. Liepold, M. Uchida, D. Willits, M. Young, T. Douglas, *Angew. Chem.* **2008**, *120*, 7963; *Angew. Chem. Int. Ed.* **2008**, *47*, 7845.

[9] C. Wang, H. Daimon, T. Onodera, T. Koda, S. H. Sun, *Angew. Chem.* **2008**, *120*, 3644; *Angew. Chem. Int. Ed.* **2008**, *47*, 3588.

[10] a) Y. Li, G. P. Whyburn, Y. Huang, *J. Am. Chem. Soc.* **2009**, *131*, 15998; b) Y. J. Li, Y. Huang, *Adv. Mater.* **2010**, *22*, 1921.

[11] K. Yamamoto, T. Imaoka, W. J. Chun, O. Enoki, H. Katoh, M. Takenaga, A. Sonoi, *Nat. Chem.* **2009**, *1*, 397.

[12] J. Turkevich, R. S. M. Jr., L. Babenkova, *J. Phys. Chem.* **1986**, *90*, 4765.

[13] H. Tsuji, Method for Producing Platinum Colloid, and Platinum Colloid Produced By The Same, U.S. Patent 6455594 B1, **2002**.

[14] a) M. Allen, D. Willits, J. Mosolf, M. Young, T. Douglas, *Adv. Mater.* **2002**, *14*, 1562; b) M. T. Klem, D. Willits, D. J. Solis, A. M. Belcher, M. Young, T. Douglas, *Adv. Funct. Mater.* **2005**, *15*, 1489.

[15] T. Douglas, E. Strable, D. Willits, A. Aitouchen, M. Libera, M. Young, *Adv. Mater.* **2002**, *14*, 415.

[16] M. L. Flenniken, M. Uchida, L. O. Liepold, S. Kang, M. J. Young, T. Douglas, *Viruses Nanotechnol.* **2009**, *327*, 71.

[17] I. Mathews, M. Soltis, M. Saldajeno, G. Ganshaw, R. Sala, W. Weyler, M. A. Cervin, G. Whited, R. Bott, *Biochemistry* **2007**, *46*, 8969.
[18] S. Bauer, A. K. Schott, V. Illarionova, A. Bacher, R. Huber, M. Fischer, *J. Mol. Biol.* **2004**, *339*, 967.
[19] H. J. Chen, T. P. Ko, C. Y. Lee, N. C. Wang, A. H. J. Wang, *Structure* **2009**, *17*, 517.
[20] C. A. Wu, N. K. Lokanath, D. Y. Kim, H. J. Park, H. Y. Hwang, S. T. Kim, S. W. Suh, K. K. Kim, *Acta Crystallogr. Sect. D* **2005**, *61*, 1459.
[21] F. Raimondi, G. G. Scherer, R. Kotz, A. Wokaun, *Angew. Chem.* **2005**, *117*, 2228; *Angew. Chem. Int. Ed.* **2005**, *44*, 2190.

